https://doi.org/10.5194/gmd-2023-180
Preprint. Discussion started: 21 November 2023

Geoscientific Model Development Discussions

A 3D-Var Assimilation Scheme for Vertical Velocity with the CMA-MESO v5.0

Hong Li[1,2], Yi Yang[1], Jian Sun[3], Yuan Jiang[3], Ruhui Gan[1], Qian Xie[1]

[1]Key Laboratory of Climate Resource Development and Disaster Prevention in Gansu Province, Center for Weather Forecasting and Climate Prediction of Lanzhou University, College of Atmospheric Sciences, Lanzhou University, Lanzhou 730000, China
[2]Institute of Arid Meteorology, China Meteorological Administration, Lanzhou 730020, China
[3]China Meteorological Administration Earth System Modeling and Prediction Centre, Beijing 100081, China

Correspondence to: Yi Yang (yangyi@lzu.edu.cn)

Abstract. Certain vertical motions associated with meso-microscale systems are favorable for convection development and maintenance; correct initialization of updraft motions is thus significant in convective precipitation forecasts. A three-dimensional variational-based vertical velocity (w) assimilation scheme has been developed within the high-resolution (3 km) CMA-MESO (the Mesoscale Weather Numerical Forecast System of China Meteorological Administration) model. This scheme utilizes the adiabatic Richardson equation as the observation operator for w, enabling the update of horizontal winds and mass fields of the model's background. The tangent linear and adjoint operators are subsequently developed and undergo an accuracy check. A single-point w observation assimilation experiment reveals that the observational information is effectively spread both horizontally and vertically. Specifically, the assimilation of w contributes to the generation of horizontal wind convergence at lower model levels and divergence at higher model levels, thereby adjusting the locations of convection occurrence. The impact of assimilating w on the convective precipitation forecast is then examined using a heavy rainfall event, and the results suggest that better 6-h precipitation forecasts are obtained by assimilating w. A batch continuous run is also conducted, and the result indicates that the scheme exhibits a high degree of robustness, leading to improved equitable threat score (frequency skill score) for the first 1 h (3 h) precipitation forecasts compared to the experiment without w assimilated.

1 Introduction

The vertical component of atmospheric motion plays a pivotal role in defining convection, as it directly influences the formation and development of clouds along with their associated precipitation. In numerical models, vertical motions are of utmost importance in parameterizing cloud dynamics and microphysical processes. This significance stems from their ability to describe the coupling between atmospheric dynamics and cloud formation and development. Consequently, they hold a crucial position in forecasting convective-scale precipitation (see, e.g., Donner et al., 2001; Lang et al., 2007; Panosetti et al.,

https://doi.org/10.5194/gmd-2023-180
Preprint. Discussion started: 21 November 2023


Geoscientific Model Development Discussions

2019; Tao et al., 2022). A three-dimensional analysis field that accurately involves both updrafts and downdrafts holds significant promise in enhancing the forecast accuracy of convective precipitation.

The vertical velocity (w) is difficult to measure directly or estimate due to its transient nature and relatively small magnitude, which is typically a few orders of magnitude smaller than the mesoscale horizontal velocities (Lee et al., 2003; Tarry et al., 2022). The well-known direct measurement is the research aircraft (e.g., LeMone and Zipser. 1980; Houze and Betts 1981; Rodts et al., 2003; Anderson et al., 2005; May et al., 2008; Heymsfield et al., 2010) but with limited spatial and temporal coverage. Besides, the nature of vertical velocities allows they can be inferred from balanced dynamics. The widely acknowledged inference of such is the so-called "continue equation", from which the w pseudo-observations are derived from horizontal divergence or convergence (Bellamy 1949; Cifelli et al., 1996). Based on the above principle or other algorithms (e.g., Williams, 2012), the w values can also be retrieved from remote sensing instruments, such as wind profilers and scanning Doppler radars (e.g., Lee et al., 2003; Liu et al., 2005; Lee et al., 2006; Heymsfield et al., 2010; Giangrande et al., 2013; Ovchinnikov et al., 2019). Motivated by the development of observation instruments and inversion algorithms of vertical velocity, more and more updrafts and downdrafts velocity "observations" emerged, especially at the cloud-resolve scale (e.g., Doppler radar and lightning data), so it is necessary to evaluate the effects of w assimilation on convective-scale precipitation forecasting.

In fact, efforts have been made to assimilate dynamic information associated with atmospheric vertical motions in recent research. For example, the w information retrieved from lightning data was assimilated based on the well-defined correlation (Price and Rind, 1992) between the total lightning flash rate and the updraft velocities (Wang et al., 2020; Xiao et al., 2021; Gan et al., 2021). These studies have shown that the assimilation of w improves the water vapor and dynamic field, and thus produces better convective precipitation forecasts. It should be noted that another work by Gan et al. (2022) revealed that the assimilation of the "zero" column maximum vertical velocity can also effectively suppress spurious convections by weakening vertical motions and reducing the hydrometeors and humidity of the model. The above w assimilation attempts are based on the nudging (Wang et al., 2020), four-dimensional variational (Xiao et al., 2021), or ensemble square root filter (Gan et al., 2021, 2022) methods, which are 1) relatively difficult to apply into the operational mesoscale regional model for computing cost consideration or 2) lack of strict physical constraints except for the four-dimensional variational method.

Since the three-dimensional variational (3D-Var) method is still widely used in operations (Gustafsson et al. 2018) due to its lower computation costs and its ability to assimilate nonmodal variables, the development of a 3D-Var assimilation technique for w observation becomes necessary. Within the 3D-Var framework, assimilating w faces numerous difficulties, the most challenging of which is the establishment of an observation operator for w. By extending w as a control variable, direct assimilation of w becomes feasible, simplifying the observation operator into a mapping algorithm from model space to observation space. However, as noted by Chen et al. (2020), the imbalance between microphysical and dynamic fields may lead to excessive noise when directly assimilating vertical velocity observations as a control variable, accomplished by adding an observation term to the 3D-Var cost function. To address this issue, Chen et al. (2020) initially computed horizontal convergence (based on the mass-continuity equation) from w pseudo-observations derived from total lightning

https://doi.org/10.5194/gmd-2023-180
Preprint. Discussion started: 21 November 2023

Geoscientific Model Development Discussions

data. Subsequently, an observation operator for horizontal convergence was developed. To achieve the direct assimilation of vertical velocity while mitigating noise, a transformation observation operator, often referred to as the observation operator, is required. This operator ensures adherence to physical constraints and aims to combine the w variable and control variables for minimizing the 3D-Var cost function. In this study, the adiabatic Richardson equation (Richardson, 1922) is employed as the observation operator of w. This choice enables the simultaneous update of dynamical and mass fields, thereby promoting a more balanced final analysis. Additionally, this direct assimilation scheme avoids the inversion errors associated with an indirect assimilation approach.

In this study, a 3D-Var assimilation scheme for vertical velocity is established within the Mesoscale Weather Numerical Forecast System of China Meteorological Administration (CMA-MESO) model. The following is the outline of this study: A brief description of the basic formulation of 3D-Var and the assimilation strategy for w observation are presented in Sect. 2. In Sect. 3, a single-point observation experiment is performed to test the spread of observational information of the assimilation scheme. The effect of assimilating w observations is then assessed by a real heavy rainfall event and a 10-day continuous run, and the results are presented and discussed in Sect. 4. Finally, the main conclusions are addressed in Sect. 5.

2 Assimilation system and vertical velocity assimilation strategy

2.1 CMA-MESO 3D-Var system

In this study, the CMA-MESO model version 5.0 is used as the forecast model. CMA-MESO (Shen et al., 2020) is a nonhydrostatic regional mesoscale system with a horizontal resolution of 3 km. The vertical velocity assimilation scheme is constructed within the 3D-Var framework of the CMA-MESO model. In the traditional framework of a variational assimilation system, the best analysis x is defined by combining the observation y^o and the background x^b by minimizing a cost function (Courtier et al., 1994):

$$J(x) = \frac{1}{2}(x - x^b)^T \boldsymbol{B}^{-1}(x - x^b) + \frac{1}{2}(H(x) - y^o)^T \boldsymbol{R}^{-1}(H(x) - y^o), \quad (1)$$

where matrices $\boldsymbol{B}$ and $\boldsymbol{R}$ represent covariances associated with background and observation errors. The matrix $\boldsymbol{B}$ is statistically based on National Meteorological Center method, and the control variables are zonal and meridional wind, pseudo-relative humidity, temperature, and surface pressure.

2.2 Observation operator for vertical velocity

H in Eq. (1) denotes the observation operator, which is used to derive the model equivalent of the observations from the model variables by the physical conversion of the assimilated variables to the control variables (Kalnay, 2002). In this study, the adiabatic Richardson equation (Richardson, 1922) is hired as the observation operator to assimilate w observation directly:

$$\gamma P \frac{\partial w}{\partial z} = -\gamma P \nabla \cdot V_h - V_h \cdot \nabla P + g \int_z^\infty \nabla \cdot (\rho V_h) dz, \quad (2)$$

https://doi.org/10.5194/gmd-2023-180
Preprint. Discussion started: 21 November 2023

Geoscientific Model Development Discussions

where γ is the ratio of specific heat capacities of air at a constant pressure (c_p) and at a constant volume (c_v), P is pressure, z is the height, V_h is the horizontal winds (components u and v), g is acceleration due to gravity and ρ is density. The Richardson equation combines the continuity equation, adiabatic equations, and hydrostatic relation, which adjust the dynamic and mass fields simultaneously and result in a more balanced analysis field. As the terrain-following vertical coordinate (Gal-Chen and Somerville, 1975) used in the CMA-MESO model is expressed as:

$$\hat{z} = z_T \frac{z - Z_s(x,y)}{Z_T - Z_s(x,y)}, \tag{3}$$

here, z_T is the top of the model upper boundary and z_s is the topographic height, the Eq. (2) in the terrain-following vertical coordinate can be expressed as:

$$\gamma\Pi^{\kappa}\frac{\Delta Z_s}{Z_T}\frac{\partial \hat{w}}{\partial z} = -\left(u\frac{\partial \Pi^{\kappa}}{\partial x} + v\frac{\partial \Pi^{\kappa}}{\partial y}\right) + \frac{\Delta Z_z}{\Delta Z_s}\left(\frac{\partial Z_s}{\partial x} + \frac{\partial Z_s}{\partial y}\right)\frac{\partial \Pi^{\kappa}}{\partial z} - \gamma\Pi^{\kappa}\left(\frac{\partial u}{\partial x} + \frac{\partial v}{\partial y}\right) - \gamma\Pi^{\kappa}\frac{\partial}{\partial z}\left(\frac{\Delta Z_z}{\Delta Z_s}\right)\left(u\frac{\partial Z_s}{\partial x} + v\frac{\partial Z_s}{\partial y}\right) - \int_z^{\infty}\frac{\partial \Pi^{\kappa}}{\partial z}\left(\frac{\partial u}{\partial x} + \frac{\partial v}{\partial y}\right)dz - \int_z^{\infty}\left(u\frac{\partial}{\partial x}\left(\frac{\partial \Pi^{\kappa}}{\partial z}\right) + v\frac{\partial}{\partial y}\left(\frac{\partial \Pi^{\kappa}}{\partial z}\right)\right)dz + \int_z^{\infty}\frac{\Delta Z_z}{\Delta Z_s}\frac{\partial \Pi^{\kappa}}{\partial z}\left(\frac{\partial Z_s}{\partial x}\frac{\partial u}{\partial z} + \frac{\partial Z_s}{\partial y}\frac{\partial v}{\partial z}\right)dz + \int_z^{\infty}\frac{\Delta Z_z}{\Delta Z_s}\frac{\partial}{\partial z}\left(\frac{\partial \Pi^{\kappa}}{\partial z}\right)\left(u\frac{\partial Z_s}{\partial x} + v\frac{\partial Z_s}{\partial y}\right)dz, \tag{4}$$

where u and v are the zonal and meridian wind components. Π is the dimensionless pressure, and $\Pi = \left(\frac{P}{P_0}\right)^{R/c_p}$, $P_0 = 1000$ hPa, and R is the gas constant. $\kappa = {c_p}/{R}$. ΔZ_s and ΔZ_z in Eq. (4) are defined as follows:

$$\Delta Z_s = Z_T - Z_s(x,y), \tag{5}$$

$$\Delta Z_z = Z_T - z(x,y), \tag{6}$$

$\hat{w}$ in Eq. (4) is the vertical velocity under the terrain-following vertical coordinate and is expressed as:

$$\hat{w} = \frac{d\hat{z}}{dt} = \frac{Z_T}{\Delta Z_s}\left(w - \frac{\Delta Z_z}{\Delta Z_s}w_s\right), \tag{7}$$

where w_s is the vertical velocity at the surface and $w_s = u\frac{\partial Z_s}{\partial x} + v\frac{\partial Z_s}{\partial y}$.

The observation operator links the w variable to the u, v, and Π variables. u and v are control variables, and Π is related to the surface pressure (control variable). Thus, as the vertical velocity assimilated through the Eq. (4), the vertical velocity of the initial field is not updated directly, but the horizontal winds and pressure fields are updated. Since the w observation term is added as a new kind of observation to the cost function of the 3D-Var system within the CMA-MESO model, modifications made to the existing 3D-Var system include the following: 1) the observation operator for w is established to calculate observation innovation; 2) the tangent linear of the observation operator for the w term is included to calculate the value of the cost function; and 3) the adjoint of the tangent linear for the w term is included to calculate the gradient value of the cost function.

2.3 Accuracy check

After completion of the vertical velocity observation operator, the correctness of the adjoint operator should be checked. For the tangent linear H' and adjoint H^T of an observation operator, the following formula is always satisfied:

https://doi.org/10.5194/gmd-2023-180
Preprint. Discussion started: 21 November 2023

Geoscientific Model Development Discussions

$$< H'(\delta x), H'(\delta x) >=< H^T\big(H'(\delta x)\big), \delta x >, \quad (8)$$

where δx represents a small perturbation and < > stands for the inner product of the vectors. The test result shows that term $< H'(\delta x), H'(\delta x) >$ is equal to 0.100159014620902D-17 (D: double precision), term $< H^T\big(H'(\delta x)\big), \delta x >$ is equal to 0.100159014620902D-17, and the difference between the two terms is 0.577778983316171D-33. As a result, the adjoint test has successfully passed under double precision.

For a tangent linear operator, it is also necessary to verify the correctness of the gradient using the following standard:

$$\Phi(\alpha) = \frac{J(c_v+\alpha)-J(c_v)}{\alpha \nabla J(c_v)}, \quad (9)$$

where c_v represents the control variable, J is the cost function, and ∇J is the gradient of J. The symbol α indicates a small value closer to zero, and the value of $\Phi(\alpha)$ is expected to be near 1. The results are presented in Table 1, showing that the tangent linear equation is accurate within the rounding error of the computer.

Table 1. Verification of gradient correctness: values of $\Phi(\alpha)$ for different α values (symbols defined in Eq. (9)).

α	$\Phi(\alpha)$
10^{-4}	1.00000684582308
10^{-5}	1.00000068454433
10^{-6}	1.00000006939151
10^{-7}	1.00000000569911
10^{-8}	1.00000003421803
10^{-9}	1.00000055706492
10^{-10}	1.00000626084813
10^{-11}	1.00001576715311
10^{-12}	1.00053861393468
10^{-13}	0.998162037654562

3 Single-point observation experiment

To investigate the spatial propagation of pseudo-observation information for variable w, a single w pseudo-observation is assimilated to assess the changes in various variables. This pseudo-observation of w is positioned at an altitude of 5448.6 m (23th model level, approximately 500 hPa) at coordinates (38.0° N, 115.2° E) (depicted as solid white or black dots in Fig. 1) with a value of 1 m s^{-1}. The observation error is set to 0.5 m s^{-1}. The background field's w value at this location is -0.04 m s^{-1}, resulting in an innovation (observation minus background) of approximately 1.04 m s^{-1}.

https://doi.org/10.5194/gmd-2023-180
Preprint. Discussion started: 21 November 2023

Geoscientific Model Development Discussions

The analysis increment induced by this observation is depicted in Fig. 1. The computed analysis increments of the horizontal wind field and its convergence at the 13th (~850 hPa) or 27th (~400 hPa) model level exhibit an isotropic structure centered around the observation site. Since a positive vertical velocity value is assimilated, a horizontal wind convergence increment is observed at the lower (13th) model level, while a horizontal wind divergence increment occurs at the middle (27th) model level. As the vertical velocity observation operator is not directly linked to temperature and specific humidity but is instead related to dimensionless air pressure, adjustments to temperature and humidity are achieved through weak physical constraints, resulting in relatively small increments in temperature and specific humidity.

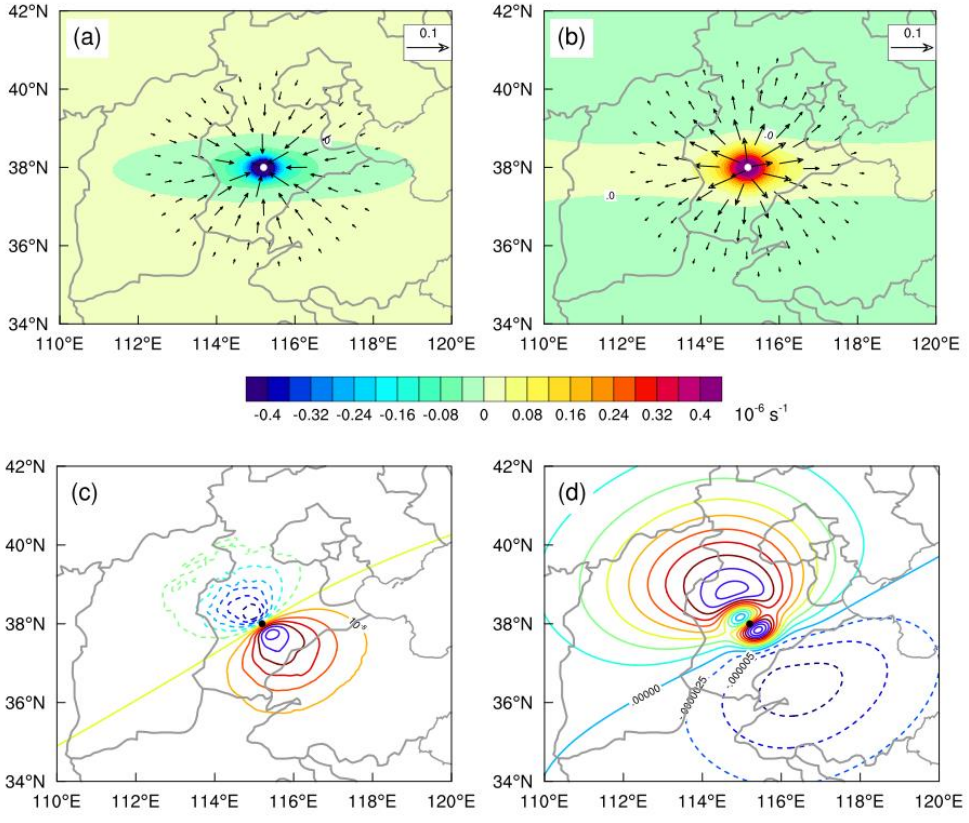

Figure 1: Analysis increments of different variables at 1500 UTC on July 4, 2020, for the single observation experiment. (a) Horizontal wind (vector; only values greater than 0.01 are shown; unit: m s^{-1}) and horizontal wind divergence (color; unit: 10^{-6} s^{-1}) increments at the 13th (~850 hPa) level of the model; (b) is the same as (a) but for the 27th (~400 hPa) level of the model. (c) Specific humidity (interval is 10^{-8}; unit: kg kg^{-1}) and (d) temperature (interval is 2.5×10^{-6} K) increments at the 13th level of the model. The solid white (black) dots in (a) and (b) ((c) and (d)) indicate the locations of the single *w* observation (38.0° N, 115.2° E).

4 Validation

In this section, a heavy rainfall event that took place on July 4, 2020, in Hebei Province is utilized to evaluate the influence of assimilating vertical velocity observations on convective analysis and precipitation forecasting. Additionally, a continuous experiment is conducted from July 1 to 10, 2020, to facilitate further testing. The pseudo-vertical velocity observations used

https://doi.org/10.5194/gmd-2023-180
Preprint. Discussion started: 21 November 2023

Geoscientific Model Development Discussions

in this study are derived from radar reflectivity. Notably, the assimilation experiment's scope can be extended to encompass vertical velocity that is observed or retrieved from alternative sources.

The radar data employed to derive pseudo-observations of w are sourced from the China Next-Generation Weather Radar (CINRAD) network and subjected to quality control procedures. Radar reflectivity serves as an indicator of convection intensity, while vertical velocity determines the vigor of convection. Radar reflectivity encompasses information about updraft motion, making it suitable for deriving pseudo-observations of w. Given that the vertical profile of w within the convective zone assumes a parabolic shape (Yuter and Houze, 1995; Collois et al., 2013; Schumacher et al., 2015), empirical Eq. (10), as utilized by Liu et al. (2010), can be employed to derive vertical velocities.

$$w = (\alpha \times (Z - Z_0) + \beta) \times e^{-(\lambda \times (H - H_0))^2}, \quad (10)$$

here, α, β, and λ represent coefficients, with α and β set to 0.1 and 0.3 respectively, in accordance with Liu et al. (2010). The coefficient Z_0 (which is 35 dBZ in this study) denotes the minimum reflectance factor value employed for w retrieval. H_0 signifies the height (unit: km) at which the maximum vertical velocity value is attained, while λ defines the primary distribution range of w in the vertical direction.

The precipitation observations used to evaluate the model forecast performance are sourced from a merged hourly 0.1°×0.1° precipitation grid dataset, combining data from China's automatic stations and the Climate Prediction Center morphing technique (CMORPH) satellite precipitation data.

4.1 The heavy rainfall case study

4.1.1 Experimental design

The simulation domain is centered at (33.5° N, 118.5° E) and employs 1101×1101 grid points in the horizontal direction, with a grid spacing of 0.03° (~3 km). The vertical dimension is represented by 49 levels extending to a model top of 35 km. Initial and lateral boundary conditions are from the National Centers for Environmental Prediction (NCEP) Global Forecast System (GFS) data. The WSM 6-class microphysics scheme (Hong and Lim, 2006), the Dudhia shortwave radiation scheme (Dudhia, 1989), the Rapid Radiative Transfer Model (RRTM) longwave radiation scheme (Mlawer et al., 1997), and the New Medium Range Forecast (NMRF) planetary boundary layer scheme (Han and Pan, 2006) is adopted. Additionally, cumulus parameterization is not utilized in these simulations.

Table 2. A brief description of experiments for the heavy rainfall case in Hebei Province.

Experiment name	Description
CTRL	Initialized at 0600 UTC on July 4, 2020, and run for 15 hours.
DA-W	The same as for the CTRL experiment, but

https://doi.org/10.5194/gmd-2023-180
Preprint. Discussion started: 21 November 2023


Geoscientific Model Development Discussions

	pseudo-observations of *w* are cyclically assimilated with an interval of 1 h from 1200 to 1500 UTC on July 4, 2020.

This heavy rainfall event occurred in the presence of a cold trough at 500 hPa. Concurrently, mild wind shear was observed, accompanied by a prevailing warm and humid airflow at 850 hPa. The precipitation mainly took place between 1300 and 2100 UTC on July 4, 2020, for this case study. Table 2 provides a concise overview of the experimental design for this case. The control experiment (CTRL) utilizes direct model forecasts, while the assimilation experiment (DA-W) incorporates the cyclic assimilation of pseudo-observations for *w*.

4.1.2 Results

Figure 2 shows the 3-h composite radar reflectivity (CR) forecasts from the CTRL and DA-W experiments. In comparison to the observed CR, the CTRL experiment displays a more southwest-oriented and stronger areal coverage of intense CR (> 35 dBZ) than the actual observations. Through the assimilation of *w* pseudo-observations (DA-W experiment), although the coverage of strong CR is less extensive than observed, the predicted locations of strong CR exhibit significant improvement. Particularly within the first hour of the forecast, both the intensity and coverage area of strong CR have notably improved.

https://doi.org/10.5194/gmd-2023-180
Preprint. Discussion started: 21 November 2023

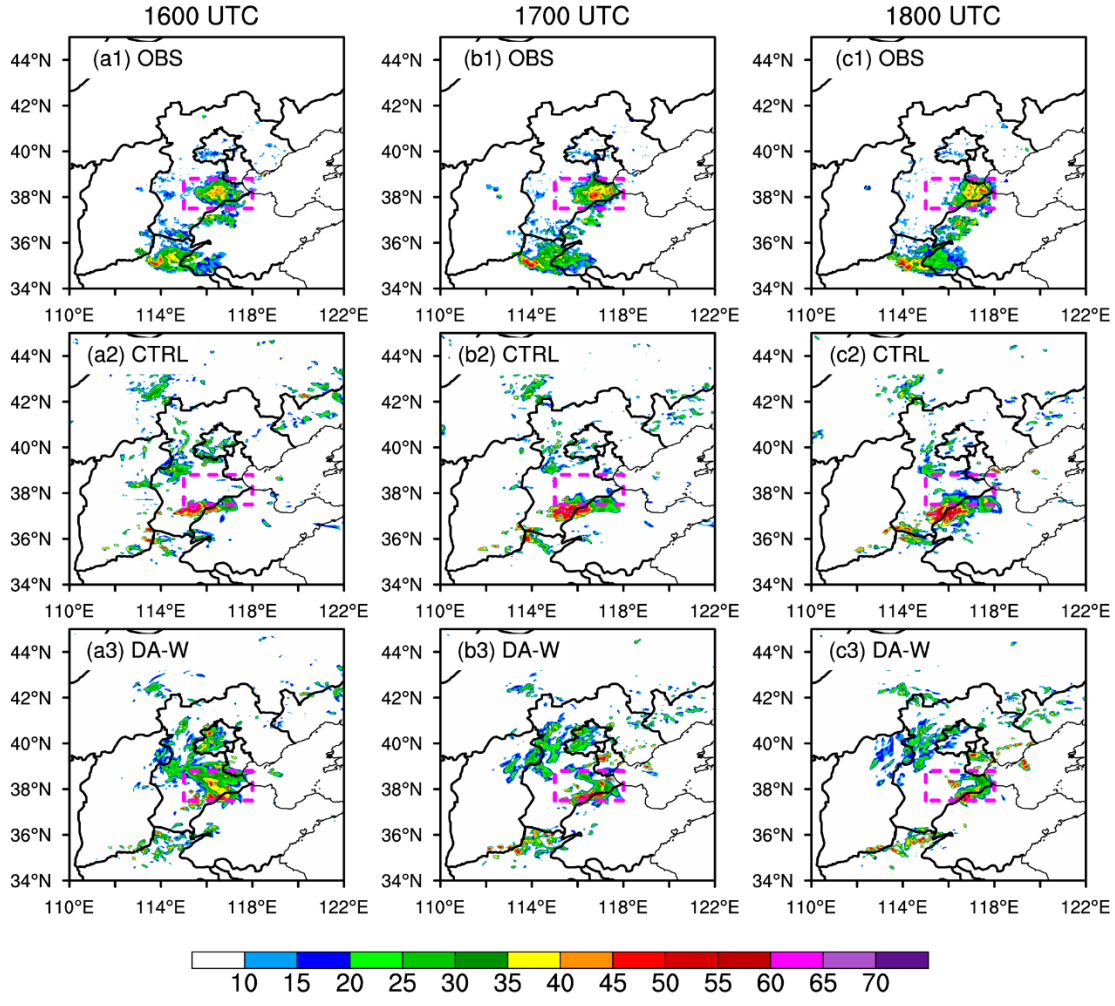

Figure 2: The observed (OBS) composite radar reflectivity (units: dBZ) and the forecast composite radar reflectivity of the (a2)–(c2) CTRL and (a3)–(c3) DA-W experiments at (a1)–(a3) 1600 UTC, (b1)–(b3) 1700 UTC, and (c1)–(c3) 1800 UTC on 4 July, 2020.

To statistically evaluate the performance of the CTRL and DA-W experiments for convective precipitation forecasting, the equitable threat score (ETS; Gandin and Murphy, 1992), the neighborhood-based fractions skill score (FSS; Roberts and Lean, 2008), and the bias score (BIAS; Anthes, 1983) are calculated for the forecast hourly accumulated precipitation. Forecasts with higher ETS (close to 1) and FSS (close to 1) and lower BIAS (closer to 1), demonstrate better forecast skills. As depicted in Fig. 3, the CTRL experiment exhibits poor 6-h precipitation forecasts, with ETS and FSS scores near zero for various thresholds. The DA-W experiment demonstrates comparatively better performance (higher ETS and FSS scores) than the CTRL experiment for thresholds of 1, 5, and 20 mm h^{-1} within the 6-h precipitation forecasts. Both experiments yield wetter forecasts (BIAS scores greater than 1), as indicated by their BIAS scores. Although the DA-W experiment produces worse BIAS scores than the CTRL experiment for thresholds of 1 and 5 mm h^{-1}, it achieves improved BIAS scores for a threshold of 20 mm h^{-1}.

https://doi.org/10.5194/gmd-2023-180
Preprint. Discussion started: 21 November 2023

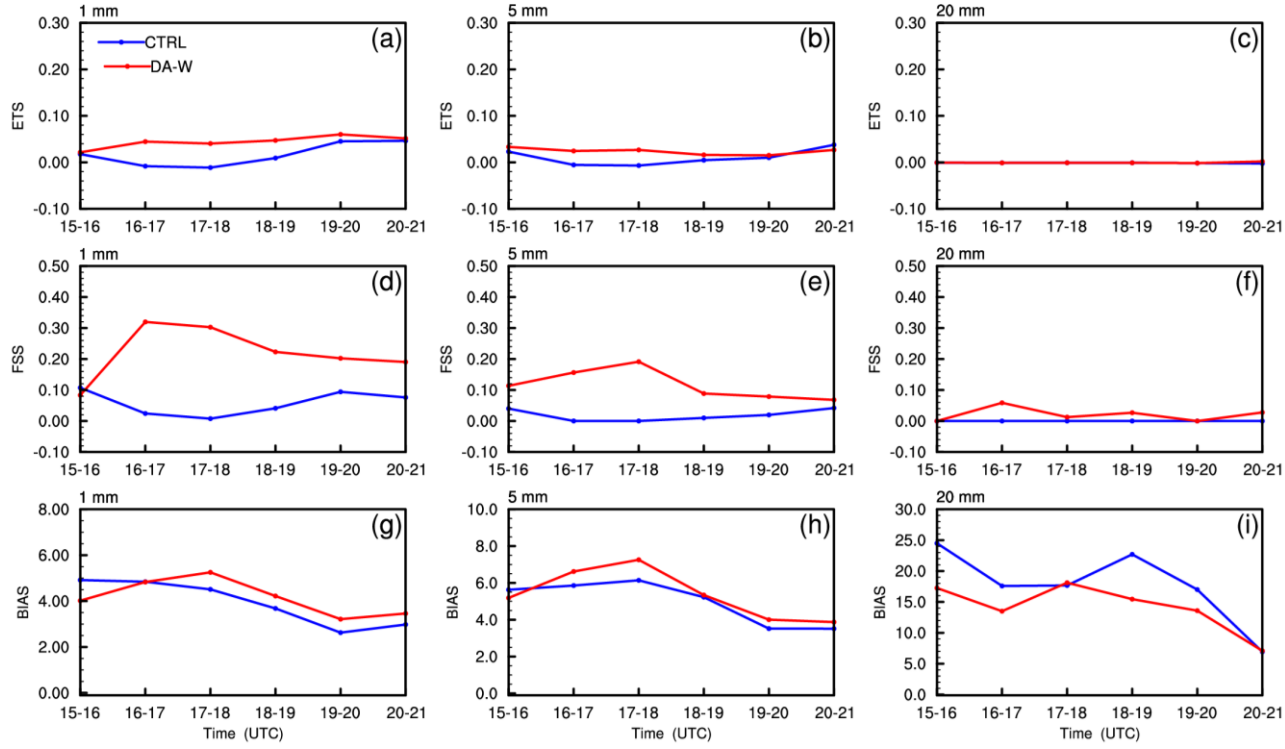

Figure 3: The equitable threat score (ETS; (a)–(c)), the neighborhood-based fractions skill score (FSS; (d)–(e)), and the bias score (BIAS; (g)–(i)) of the predicted hourly accumulated precipitation of the CTRL and DA-W experiments for thresholds of 1 mm h^{-1}, 5 mm h^{-1}, and 20 mm h^{-1} for the heavy rainfall case on 4 July 2020.

4.2 The batch experiment

The case study presented in Sect. 4.1 demonstrates the potential of assimilating *w* pseudo-observations to improve convective-scale precipitation forecasting. To further assess the assimilation impact of *w* pseudo-observations, a continuous 10-day run spanning from July 1 to July 10, 2020, was conducted. Unlike the case study, the simulation area for the batch experiment corresponds to the operational area of the CMA-MESO model (refer to Fig. 4 (a)), centered at coordinates (35.05° N, 107.5° E). The horizontal grid comprises 2501×1671 grid points. Similarly, two distinct experiments were configured, and an overview of the experimental setup is depicted in Fig. 4 (b). Both the CTRL and DA-W experiments were initialized at 0600 UTC from July 1 to July 10, 2020, and were run for 12 hours each. While the CTRL experiment assimilates observations from aircraft measurements, radiosondes, and other sources (for a comprehensive list, refer to Fig. 4 (b)) at the initial time, the main distinction in the DA-W experiment is the assimilation of *w* pseudo-observations.

https://doi.org/10.5194/gmd-2023-180
Preprint. Discussion started: 21 November 2023

Geoscientific Model Development Discussions
Open Access
EGU

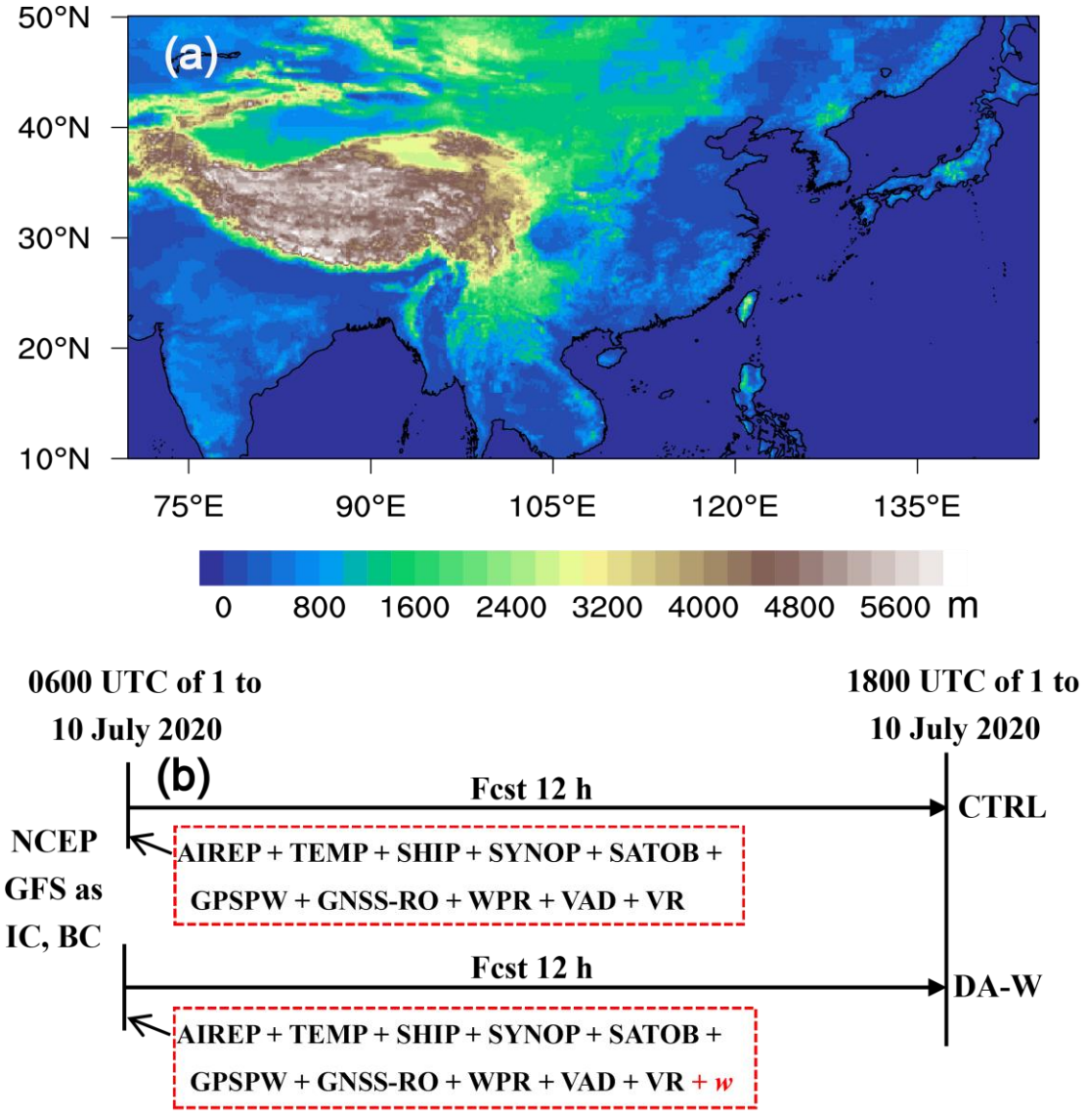

Figure 4: The simulation domain (a) and the numerical experimental scheme (b) for the CTRL and DA-W batch experiments. Both experiments use NCEP GFS data as the initial condition (IC) and boundary condition (BC). The symbol "Fcst" means forecast. The assimilated data comprises conventional observations from aircraft measurements (AIREP), radiosondes (TEMP), ships (SHIP), and ground stations (SYNOP). In addition, cloud-track-wind (SATOB), precipitable water derived from the Global Positioning System (GPSPW), refractivity radio-occultation data from the Global Navigation Satellite System (GNSS-RO), wind profiler radar (WPR), velocity-azimuth display (VAD) wind, and the radar radial velocity (VR). The pseudo-vertical velocity (*w*) data are also assimilated for the DA-W experiment.

The forecast skills (ETS and FSS) for hourly accumulated precipitation in the 12-h predictions, initialized at 0600 UTC each day, are presented in Fig. 5 and Fig. 6. It is evident that the ETS of the DA-W experiment shows immediate improvement (or remains the same as that of the CTRL experiment) within the first 1-h forecast across all days. This indicates the immediate

https://doi.org/10.5194/gmd-2023-180
Preprint. Discussion started: 21 November 2023

Geoscientific Model Development Discussions

positive impact of assimilating *w* pseudo-observations on the forecasts. As the forecast lead time progresses, the scores of the two experiments gradually approach each other. In terms of FSS, the DA-W experiment exhibits notable score improvement within the first 3-h forecast for thresholds of 1, 5, and 20 mm h^{-1}, except for predictions initialized at 0600 UTC on July 2, 2020 (Fig. 6 (a2) – (c2)). This suggests that assimilating *w* pseudo-observations has a positive effect on the forecast precipitation position.

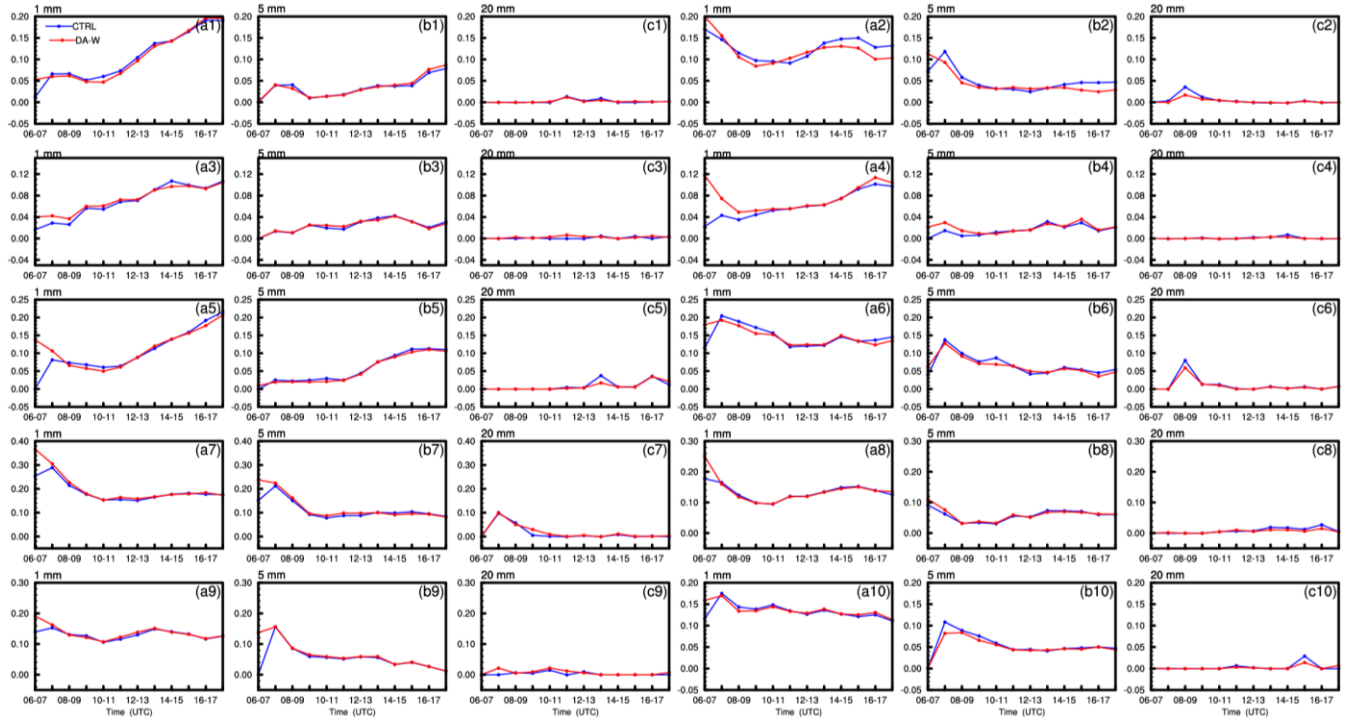

Figure 5: The equitable threat score (ETS) of the predicted hourly accumulated precipitation of the CTRL and DA-W experiments for thresholds of 1 mm h^{-1} ((a1)–(a10)), 5 mm h^{-1} ((b1)–(b10)), and 20 mm h^{-1}((c1)–(c10)) for the continuous run on different days. For example, (a1)–(c1) are scores for the prediction initialized at 0600 UTC on 1 July 2020.

https://doi.org/10.5194/gmd-2023-180
Preprint. Discussion started: 21 November 2023

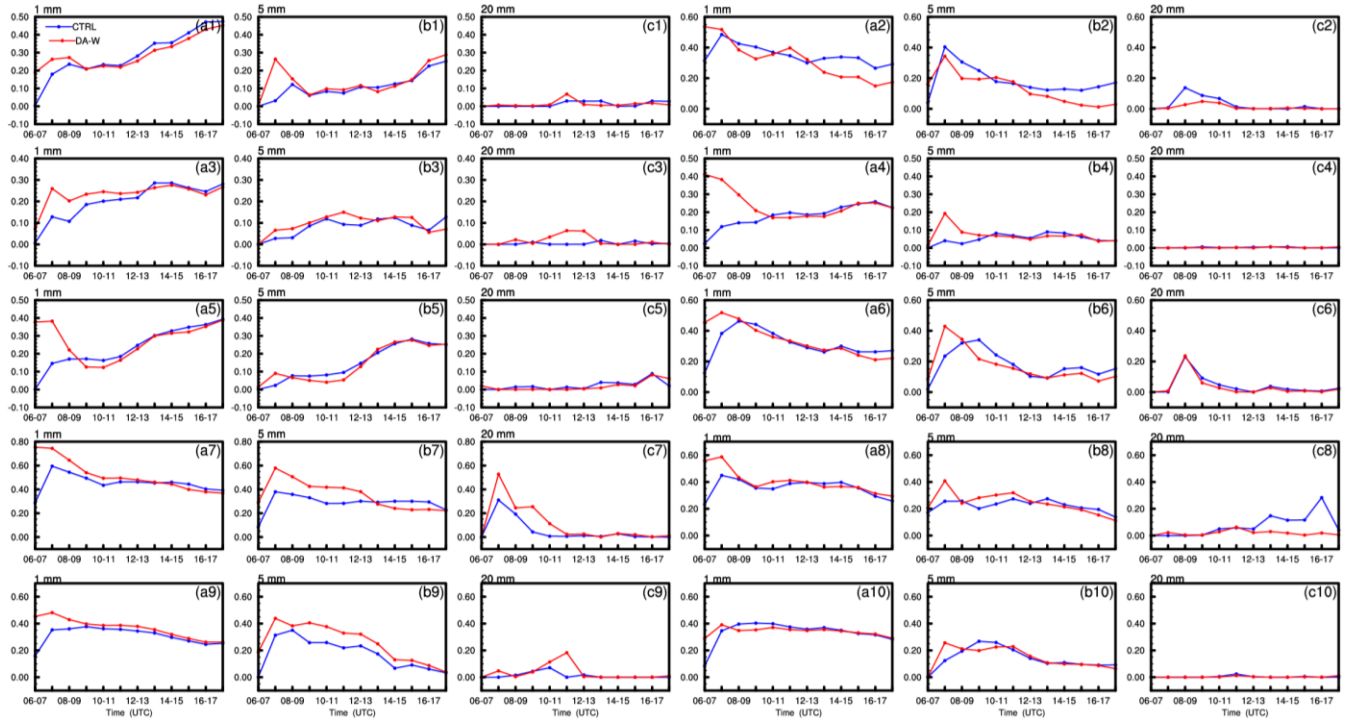

Figure 6: Same as Fig. 5 but for the neighborhood-based fractions skill score (FSS).

5 Conclusions and discussion

Dynamical processes, especially vertical air motions, play a crucial role in convective precipitation forecasts as they contribute to the development of clouds and precipitation. In this study, a 3D-Var data assimilation scheme for vertical velocity (w), based on the adiabatic Richardson equation, is developed within the high-resolution (3 km) CMA-MESO model. The CMA-MESO 3D-Var system employs the horizontal wind components u and v as momentum control variables. The observation operator for w establishes the relationship between w and u, v, as well as Π (dimensionless air pressure). This allows the u and v fields to be updated directly by assimilating w observations. The results of the single observation test indicate a reasonable distribution of horizontal wind increments. Specifically, horizontal wind convergence (resulting from assimilating a positive value of w) is observed at the lower model level (~850 hPa), while horizontal wind divergence tends to occur at the higher model level (~400 hPa). These adjustments effectively contribute to the establishment or reinforcement of convection in these areas.

The impact of assimilating pseudo-observations of w on analysis and precipitation forecasts is then investigated through the study of a heavy rainfall event in Hebei Province and a continuous10-day experiment. In the heavy rainfall case, the spatial distribution of composite radar reflectivity forecast from the DA-W experiment (where retrieved pseudo-observations of w are assimilated at a 1-h interval during a 3-h data assimilation period) shows significant improvement compared to the CTRL

https://doi.org/10.5194/gmd-2023-180
Preprint. Discussion started: 21 November 2023


Geoscientific Model Development Discussions

experiment (where no observations are assimilated). This leads to better FSS and ETS scores in 6-h precipitation forecasts. The results from the continuous run experiment demonstrate that assimilating pseudo-observations of *w* contributes to improved precipitation position forecasts, as reflected in higher FSS scores for thresholds of 1, 5, and 20 mm h^{-1} during the initial 3-h forecasts.

Our study has successfully achieved the direct assimilation of vertical velocity within the current CMA-MESO 3D-Var system, yielding promising preliminary results. However, there are certain limitations that cannot be overlooked and require further attention. For instance: 1) The current approach does not take into account the cross correlation between different control variables of the matrix $\boldsymbol{B}$. The adjustments in temperature and humidity increments are achieved by weak physical constraints. However, the analysis field is significantly affected by the matrix $\boldsymbol{B}$ (Navon et al., 2005). 2) The pseudo-observations of *w* used in this study are derived from radar reflectivity. While radar reflectivity observations have traditionally been employed to initialize the moisture field and hydrometeors of regional models (e.g., Albers et al. 1996; Sun and Crook, 1997; Hu et al., 2006; Wang et al., 2013; Lai et al., 2019; Liu et al., 2022), the benefits of assimilating high-resolution radar data might diminish due to inconsistencies in dynamic information. It is imperative to concurrently update dynamical variables in order to maintain a balanced initial field. Our approach could potentially address this issue, given that direct assimilation of *w* observations is possible. As the CMA-MESO model progresses in incorporating radar reflectivity factor assimilation, the combined assimilation of water vapor, hydrometeors, and vertical velocity warrants further exploration.

Code availability

The CMA-MESO v5.0 source code is provided by the Chinese Meteorological Administration and cannot be publicly available due to the copyright license requirement from the China Meteorological Administration Earth System Modeling and Prediction Centre (CEMC). If someone wish to acquire the code to reproduce the study, please contact the operational management department of the CEMC via email (sunqin@cma.gov.cn) or phone (+86-10-58994128). The code of the observation operator, the tangent linear of the observation operator, and the adjoint operator for vertical velocity is available at https://doi.org/10.5281/zenodo.10073822.

Data availability

The model outputs from the “Single-point observation experiment” and “The heavy rainfall case study” sections, along with the processed data from the “The batch experiment” section of the paper, are available at https://doi.org/10.5281/zenodo.8300610. The NCEP GFS data used are available at https://rda.ucar.edu/datasets/ds084.1/.

https://doi.org/10.5194/gmd-2023-180
Preprint. Discussion started: 21 November 2023

The raw Doppler radar and precipitation observations are provided by the Chinese Meteorological Administration and can be obtained via request from http://www.cma.gov.cn/en2014/.

Author Contributions

Yi Yang conceived the idea and designed the research. Hong Li performed the research and wrote the first draft of the manuscript. All authors discussed the results and contributed to writing and revisions.

Conflict of interest

The authors declare no conflicts of interest or competing financial interests.

Acknowledgments

The authors gratefully acknowledge the CEMC for providing the source code of CMA-MESO v5.0. Additionally, the authors appreciate the NCEP for providing the GFS data and the Chinese Meteorological Administration for providing the radar and precipitation data. Furthermore, special thanks to the Supercomputing Center of Lanzhou University for computational support.

Financial support

This study was jointly supported by the Youth Science and Technology Foundation Program of Gansu Province (23JRRA1327), the National Natural Science Foundation of China (42205050), and the Gansu Provincial Association of Science and Technology Innovation Drive Promotion Project (GXH20230817-7).

References

Albers, S. C., McGinley, J. A., Birkenheuer, D. A., and Smart, J. R.: The local analysis and prediction system (LAPS): Analysis of clouds, precipitation and temperature, Wea. Forecasting, 11, 273–287, doi:10.1175/1520-0434(1996)011<0273:TLAAPS>2.0.CO;2, 1996.

Anderson, N. F., Grainger, C. A., and Stith, J. L.: Characteristics of strong updrafts in precipitation systems over the central tropical Pacific Ocean and in the Amazon, J. Appl. Meteorol., 44, 731–738, doi:10.1175/JAM2231.1, 2005.

Anthes, R. A.: Regional Models of the Atmosphere in Middle Latitudes, Mon. Wea. Rev., 111(6), 1306–1335, doi:10.1175/1520-0493(1983)111<1306:rmotai>2.0.co;2, 1983.

https://doi.org/10.5194/gmd-2023-180
Preprint. Discussion started: 21 November 2023

Bellamy, J. C.: Objective calculations of divergence, vertical velocity and vorticity, Bull. Amer. Meteor. Soc., 30, 45–49, 1949.

Chen, Z., Sun, J., Qie, X., Zhang, Y., Ying, Z., Xiao, X., and Cao, D.: A method to update model kinematic states by assimilating satellite-observed total lightning data to improve convective analysis and forecasting, J. Geophys. Res. Atmos., 125(22), 1–26, doi:10.1029/2020jd033330, 2020.

Cifelli, R., Rutledge, S. A., Boccippio, D. J., and Matejka, T.: Horizontal Divergence and Vertical velocity Retrieval from Doppler Radar and Wind Profiler observations, J. Atmos. Ocean. Tech., 13, 948–966, doi:10.1175/1520-0426(1996)013<0948:HDAVVR>2.0.CO;2, 1996.

Collis, S., Protat, A., May, P. T., and Williams, C.: Statistics of storm updraft velocities from TWP-ICE including verification with profiling measurements, J. Appl. Meteorol. Clim., 52, 1909–1922, doi:10.1175/JAMC-D-12-0230.1, 2013.

Courtier, P., Thepaut, J.-N., and Hollingsworth, A.: A strategy for operational implementation of 4D-Var, using an incremental approach, Q. J. R. Meteorol. Soc., 120, 1367–1387, doi:10.1002/qj.49712051912, 1994.

Donner, L. J., Seman, C. J., Hemler, R. S., and Fan, S.: A Cumulus Parameterization Including Mass Fluxes, Convective Vertical Velocities, and Mesoscale Effects: Thermodynamic and Hydrological Aspects in a General Circulation Model, J. Atmos. Sci., 14, 3444–3463, doi:10.1175/1520-0442(2001)014<3444:ACPIMF>2.0.CO;2, 2001.

Dudhia, J.: Numerical study of convection observed during the winter monsoon experiment using a mesoscale two-dimensional model, J. Atmos. Sci. 46(20), 3077–3107, doi:10.1175/1520-0469(1989)046<3077:nsocod>2.0.co;2, 1989.

Gal-Chen, T. J. and Somerville, R. C.: On the use of a coordinate transformation for the resolution of the Navier-Stokes equation, J. Comput. Phys., 17, 209–228, doi:10.1016/0021-9991(75)90037-6, 1975.

Gan, R., Yang, Y., Qiu, X., Wang, R., Qiu, X., and Zhu, L.: Assimilation of the maximum vertical velocity converted from total lightning data through the EnSRF method, J. Geophys. Res. Atmos., 126, e2020JD034300, doi:10.1029/2020JD034300, 2021.

Gan, R., Yang, Y., Qiu, X., Liu, P., Wang, X., and Gu, K.: A scheme to suppress spurious convection by assimilating the "zero" column maximum vertical velocity, J. Geophys. Res. Atmos., 127, e2021JD035536, doi:10.1029/2021JD03553, 2022.

Gandin, L. S. and Murphy, A. H.: Equitable skill scores for categorical forecasts, Mon. Wea. Rev., 120, 361–370, doi:10.1175/1520-0493(1992)120<0361:ESSFCF>2.0.CO;2, 1992.

Giangrande, S. E., Collis, S., Straka, J., Protat, A., Williams, C., and Krueger, S.: A Summary of Convective-Core Vertical Velocity Properties Using ARM UHF Wind Profilers in Oklahoma, J. Appl. Meteorol. Clim., 52(10), 2278–2295, doi:10.1175/jamc-d-12-0185.1, 2013.

Gustafsson, N. and Coauthors: Survey of data assimilation methods for convective-scale numerical weather prediction at operational centers, Quart. J. Roy. Meteor. Soc., 144, 1218–1256, doi:10.1002/qj.3179, 2018.

Han, J. and Pan, H.-L.: Sensitivity of Hurricane Intensity Forecast to Convective Momentum Transport Parameterization, Mon. Wea. Rev., 134(2), 664–674. doi:10.1175/mwr3090.1, 2006.

https://doi.org/10.5194/gmd-2023-180
Preprint. Discussion started: 21 November 2023

Heymsfield, G. M., Tian, L., Heymsfield, A. J., Li, L., and Guimond, S.: Characteristics of deep tropical and subtropical convection from nadir-viewing high-altitude airborne Doppler radar, J. Atmos. Sci., 67, 285–308, doi:10.1175/2009JAS3132.1, 2010.

Hong, S.-Y. and Lim, J.-O. J.: The WRF single-moment 6-class microphysics scheme (WSM6), J. Korean Meteor. Sci., 42, 129–151, 2006.

Houze, R. A. Jr. and Betts, A. K.: Convection in GATE, Rev. Geophys., 19, 541–576, doi:10.1029/RG019i004p00541, 1981.

Hu, M., Xue, M., and Brewster, K.: 3DVAR and cloud analysis with WSR-88D Level-II data for the prediction of the Fort Worth tornadic thunderstorms. Part I: Cloud analysis and its impact, Mon. Weather Rev., 134, 675–698, doi:10.1175/MWR3092.1, 2006.

Lai, A., Gao, J., Koch, S. E., Wang, Y., Pan, S., Fierro, A. O., Cui, C., and Min, J.: Assimilation of radar radial velocity, reflectivity, and pseudowater vapor for convective-scale NWP in a variational framework, Mon. Weather Rev., 147, 2877–2900, doi:10.1175/MWR-D-18-0403.1, 2019.

Lang, S., Tao, W.-K., Cifelli, R., Olson, W., Halverson, J., Rutledge, S., and Simpson, J.: Improving simulations of convective Systems from TRMM LBA: Easterly and Westerly Regimes, J. Atmos. Sci., 64, 1141–1164, doi:10.1175/JAS3879.1, 2007.

Lee, J. L., Kuo, Y.-H., and MacDonald, A. E.: The vorticity method: Extension to mesoscale vertical velocity and validation for tropical storms, Quart. J. Roy. Meteor. Soc., 129, 1029–1050, doi:10.1256/qj.01.219, 2003.

Lee, J. L., Lee, W. C., and MacDonald, A. E.: Estimating vertical velocity and radial flow from Doppler radar observations of tropical cyclones, Quart. J. Roy. Meteor. Soc., 132, 125–145, doi:10.1256/qj.04.77, 2006.

LeMone, M. A. and Zipser, E. J.: Cumulonimbus vertical velocity events in GATE. Part I: Diameter, intensity and mass flux, J. Atmos. Sci., 37, 2444–2457, doi:10.1175/1520-0469(1980)037<2444:CVVEIG>2.0.CO;2, 1980.

Liu, H. Y., Xue, J. S., Gu, J. F., and Xu, H. M.: GRAPES-3DVAR radar data assimilation and numerical simulation experiments with a torrential rain case, Acta Meteorological Sinica, 68(6), 779–789, 2010. (in Chinese)

Liu, P., Yang, Z. D., Wang, X. S., Qiu, X. B., and Yang, Y.: Assimilation of the pseudo-water vapor derived from extrapolated radar reflectivity to improve the forecasts of convective events, Atmos. Res., 279(3):106386, doi:10.1016/j.atmosres.2022.106386, 2022.

Liu, S., Qiu, C., Xu, Q., Zhang, P., Gao, J., and Shao, A.: An improved method for Doppler wind and thermodynamic retrievals, Adv. Atmos. Sci., 22, 90–102, doi:10.1007/BF02930872, 2005.

May, P. T., Mather, J. H., Vaughan, G., Jakob, C., McFarquhar, G. M., Bower, K. N., and Mace, G. G.: The tropical warm pool international cloud experiment, Bull. Amer. Meteor. Soc., 89, 629–645, doi:10.1175/BAMS-89-5-629, 2008.

Mlawer, E. J., Taubman, S. J., Brown, P. D., Iacono, M. J., and Clough, S. A.: Radiative transfer for inhomogeneous atmospheres: RRTM, a validated correlated-k model for the longwave, J. Geophys. Res. Atmos., 102, 16663–16682, doi:10.1029/97JD00237, 1997.

https://doi.org/10.5194/gmd-2023-180
Preprint. Discussion started: 21 November 2023

Navon, I. M., Daescu, D. N. and Liu, Z.: The impact of background error on incomplete observations for 4D-Var data assimilation with the FSU GSM, Lect. Notes Comput. Sci., 3515, 837–844, 2005.

Kalnay, E.: Atmospheric Modeling, Data Assimilation, and Predictability, Cambridge University Press, 2002.

Ovchinnikov, M., Giangrande, S., Larson, V. E., Protat, A., and Williams, C. R.: Dependence of vertical alignment of cloud and precipitation properties on their effective fall speeds, J. Geophys. Res. Atmos., 124(4), 2079–2093, doi:10.1029/2018JD029346, 2019.

Panosetti, D., Schlemmer, L., and Schär, C.: Bulk and structural convergence at convection-resolving scales in real-case simulations of summertime moist convection over land, Quart. J. Roy. Meteor. Soc., 145, 1427–1443, doi:10.1002/qj.3502, 2019.

Price, C. and Rind, D.: A simple lightning parameterization for calculating global lightning distributions, J. Geophys. Res. Atmos., 97, 9919–9933, doi:10.1029/92JD00719, 1992.

Richardson, L. F.: Weather Prediction by Numerical Process, Cambridge University Press, 236 pp, 1922.

Roberts, N.M. and Lean, H.W.: Scale-selective verification of rainfall accumulations from high-resolution forecasts of convective events, Mon.Wea. Rev., 136, 78–97, doi:10.1175/2007MWR2123.1, 2008.

Rodts, S. M. A., Duynkerke, P. G., and Jonker, H. J. J.: Size distributions and dynamical properties of shallow cumulus clouds from aircraft observations and satellite data, J. Atmos. Sci., 60, 1895–1912, doi:10.1175/1520-0469(2003)060<1895:SDADPO>2.0.CO;2, 2003.

Schumacher, C., Stevenson, S. N. and Williams, C. R.: Vertical motions of the tropical convective cloud spectrum over Darwin, Australia, Q. J. Roy. Meteor. Soc., 141, 2277–2288, doi:10.1002/qj.2520, 2015.

Shen, X. S., Wang, J. J., Li, Z. C., Chen, D. H., and Gong, J, D.: Research and operational development of numerical weather prediction in China, J. Meteor. Res., 34(4), 675–698, doi:10.1007/s13351-020-9847-6, 2020.

Sun, J. and Crook, N. A.: Dynamical and microphysical retrieval from Doppler radar observations using a cloud model and its adjoint. Part I: Model development and simulated data experiments, J. Atmos. Sci., 54, 1642–1661, doi:10.1175/1520-0469(1997)054<1642:DAMRFD>2.0.CO;2, 1997.

Tao, W.-K., Iguchi, T., Lang, S., Li, X., Mohr, K., Matsui, T., et al.: Relating vertical velocity and cloud/precipitation properties: A numerical cloud ensemble modeling study of tropical convection, J. Adv. Model. Earth Syst., 14, e2021MS002677, doi:10.1029/2021MS002677, 2022.

Tarry, D. R., Ruiz, S., Johnston, T., Poulain, P.-M., Özgökmen, T., Centurioni, L. R., et al.: Drifter observations reveal intense vertical velocity in a surface ocean front, Geophys. Res. Lett., 49, e2022GL098969, doi:10.1029/2022GL098969, 2022.

Wang, H., Chen, D., Yin, J., Xu, D., Dai, G., and Chen, L.: An improvement of convective precipitation nowcasting through lightning data dynamic nudging in a cloud-resolving scale forecasting system, Atmos. Res., 242, 1–11, doi:10.1016/j.atmosres.2020.104994, 2020.

https://doi.org/10.5194/gmd-2023-180
Preprint. Discussion started: 21 November 2023

Wang, H., Sun, J., Fan, S., and Huang, X.-Y.: Indirect assimilation of radar reflectivity with WRF 3D-Var and its impact on prediction of four summertime convective events, J. Appl. Meteorol. Climatol., 52, 889–902, doi:10.1175/JAMC-D-12-0120.1, 2013.

Williams, C. R.: Vertical air motion retrieved from dual-frequency profiler observations, J. Atmos. Ocean. Tech., 29(10), 1471–1480, doi:10.1175/jtech-d-11-00176.1, 2012.

Xiao, X., Sun, J., Qie, X., Ying, Z., Ji, L., Chen, M., and Zhang, L.: Lightning data assimilation scheme in a 4DVAR system and its impact on very short-term convective forecasting, Mon. Weather Rev., 149(2), 353–373, doi:10.1175/mwr-d-19-0396.1, 2021.

Yuter, S. E. and Houze, R. A.: Three-dimensional kinematic and microphysical evolution of Florida cumulonimbus: Part II. Frequency distribution of vertical velocity, reflectivity, and the differential reflectivity, Mon. Weather Rev., 123, 1941–1963, doi:10.1175/1520-0493(1995)123<1941:TDKAME>2.0.CO;2, 1995.